BMC Cell Biology

BioMed Central

Research article

Quantitation of the distribution and flux of myosin-II during cytokinesis

Douglas N Robinson†*[1,2], Guy Cavet†[1,3], Hans M Warrick[1] and James A Spudich[1]

Address: [1]Departments of Biochemistry and Developmental Biology, Stanford University School of Medicine, Stanford, CA 94305-5307, USA, [2]Current address: Department of Cell Biology, Johns Hopkins University School of Medicine, 725 N. Wolfe St.. Baltimore, MD 21205, USA, [3]Current address: Rosetta Inpharmatics, 12040 115th Ave NE, Kirkland, WA 98034, USA

E-mail: Douglas N Robinson* - Douglas.Robinson@jhu.edu; Guy Cavet - gcavet@rii.com; Hans M Warrick - warrick@cmgm.stanford.edu; James A Spudich - jspudich@cmgm.stanford.edu

*Corresponding author †Equal contributors

Published: 8 February 2002

BMC Cell Biology 2002, **3**:4

Received: 13 November 2001
Accepted: 8 February 2002

This article is available from: http://www.biomedcentral.com/1471-2121/3/4

Abstract

Background: During cytokinesis, the cell's equator contracts against the cell's global stiffness. Identifying the biochemical basis for these mechanical parameters is essential for understanding how cells divide. To achieve this goal, the distribution and flux of the cell division machinery must be quantified. Here we report the first quantitative analysis of the distribution and flux of myosin-II, an essential element of the contractile ring.

Results: The fluxes of myosin-II in the furrow cortex, the polar cortex, and the cytoplasm were examined using ratio imaging of GFP fusion proteins expressed in *Dictyostelium*. The peak concentration of GFP-myosin-II in the furrow cortex is 1.8-fold higher than in the polar cortex and 2.0-fold higher than in the cytoplasm. The myosin-II in the furrow cortex, however, represents only 10% of the total cellular myosin-II. An estimate of the minimal amount of this motor needed to produce the required force for cell cleavage fits well with this 10% value. The cell may, therefore, regulate the amount of myosin-II sent to the furrow cortex in accordance with the amount needed there. Quantitation of the distribution and flux of a mutant myosin-II that is defective in phosphorylation-dependent thick filament disassembly confirms that heavy chain phosphorylation regulates normal recruitment to the furrow cortex.

Conclusion: The analysis indicates that myosin-II flux through the cleavage furrow cortex is regulated by thick filament phosphorylation. Further, the amount of myosin-II observed in the furrow cortex is in close agreement with the amount predicted to be required from a simple theoretical analysis.

Background

Cellular morphogenesis is fundamental to all developmental processes and is essential for cellular proliferation. Morphogenesis depends on the interactions of steady state and dynamic physical properties that allow a cell to deform and reform into different shapes, such as neuronal growth cones and columnar epithelia. Identifying the mechanical properties of cells that allow them to undergo

shape changes and elucidating the molecular mechanisms that cells use to generate the mechanical forces remains the ultimate challenge of understanding cellular morphogenesis. One dramatic example of a process in which a cell reshapes itself is during the mechanical separation of a mother cell into two daughter cells during cytokinesis.

In an animal cell, cytokinesis involves the generation of force in the region of the contractile ring (reviewed in [1]). This was first appreciated in the 1960's when Rappaport demonstrated that the cleavage furrow cortex of echinoderm eggs produced force that was capable of bending a glass needle (reviewed in [1]). Using calibrated needles, Rappaport directly measured the force that the contractile ring produced [2]. During the 1970's, nonmuscle myosin-II, the equivalent of the force producing molecule of skeletal muscle, was shown to localize to the region of the cleavage furrow cortex, suggesting the molecular basis for contractile force (reviewed in [1,3]). Indeed, subsequent genetic studies revealed a nearly ubiquitous requirement for nonmuscle myosin-II during cytokinesis in organisms ranging from the cellular slime molds to metazoans (reviewed in [3]).

One appeal of studying cytokinesis as a model for cellular morphogenesis is its relatively simple geometry during normal mitotic cell divisions, which produce equal sized daughter cells. This theme can be modified for specific developmental programs such as the unequal cleavages of mammalian female meiosis. However, during standard mitosis, the mother cell may be modeled as a simple sphere, which is deformed in the region of its equator to mimic the ingression of the furrow. The furrow ingresses until a small intercellular bridge forms. The intercellular bridge is severed or resolved, resulting in separation of the two daughter cells. Cell division can then be thought of as a series of intermediate cell shapes (sphere, cylinder and dumbbell) that are produced along this pathway of cleaving the mother cell. Yoneda and Dan [4] suggested a model for cytokinesis based on Hooke's Law. In their model, the minimal contractile force required for stabilizing each of these intermediate shapes is proportional to the global steady state stiffness of the cell and is dependent on the extent of furrow ingression.

A quantitation of the distribution and flux of each factor is essential for developing a physical model for a cellular activity. Myosin-II recruitment to the cortex and to the cleavage furrow cortex depends on the thick filament-state of this molecular motor [5–8]. The ability to form thick filaments is regulated by phosphorylation of three threonines near the tail of the long coiled-coil. When the protein is fully phosphorylated, it remains largely in the monomeric state; whereas removal of these phosphates allows the protein to assemble into thick filaments. Substitution of the three threonines with alanines produces the 3 × Ala mutant that behaves like a constitutively unphosphorylated myosin-II. It partially rescues the myosin heavy chain (*mhcA*) null strain and localizes to the cleavage furrow cortex. A quantitative comparison of wild type and 3 × Ala myosin-II can help to constrain models about how myosin-II is recruited to the cleavage furrow cortex.

In this paper, we conduct a detailed ratio imaging study using green fluorescent protein (GFP)-labeled wild type and 3 × Ala myosin-II and a soluble GFP as a volume marker. We determine the amount of myosin-II that is in the cleavage furrow cortex and monitor the flux of wild type and 3 × Ala myosin-II during cytokinesis. We apply the simple mathematical relationship proposed by Yoneda and Dan [4] to the geometry of dividing *Dictyostelium discoideum* cells. By considering the stiffness of a *D. discoideum* cell [9,10], we estimate the minimal required force to cleave a cell as a function of the cell's geometry. We then consider the mechanical properties of myosin-II that have been measured using modern biophysical tools [11–14] to estimate how much myosin-II would be required to generate a particular amount of force. We find that the amount of myosin-II needed for cytokinesis and the amount of myosin-II that actually accumulates in the furrow region are in good agreement. This analysis provides a useful framework for relating the biochemical and biophysical properties of myosin-II to the mechanical process of cytokinesis.

Results

Ratio imaging Quantitatively measures GFP-Myosin-II dynamics

To begin to develop a physical model for cytokinesis, we analyzed the changes in the distribution of wild type myosin-II and 3 × Ala GFP-myosin-II during the cell cycle using ratio imaging. This allowed us to quantify the flux of myosin-II during cytokinesis and to examine the role of heavy chain phosphorylation in this flux. Ratio imaging is preferred to other types of microscopy for determining local concentrations of a protein of interest because the whole cell is considered simultaneously and the signal is normalized to a volume indicator.

To perform ratio imaging of GFP-myosin-II, it was expressed in a myosin-II heavy chain (*mhcA*) mutant strain where it completely rescued the mutant. It was co-expressed with a second form of GFP fused to a nuclear localization signal (NLS-GFP). These two GFP variants, GFP-Vex1 and GFP-Bex1 [15], have distinct excitation spectra so that separate images can be obtained for the two fusion proteins and used to generate ratio images. Since NLS-GFP is relatively large (27 kDa), we examined the uniformity of its distribution by comparing it to a Texas Red-labeled dextran with a 4 kDa molecular weight.

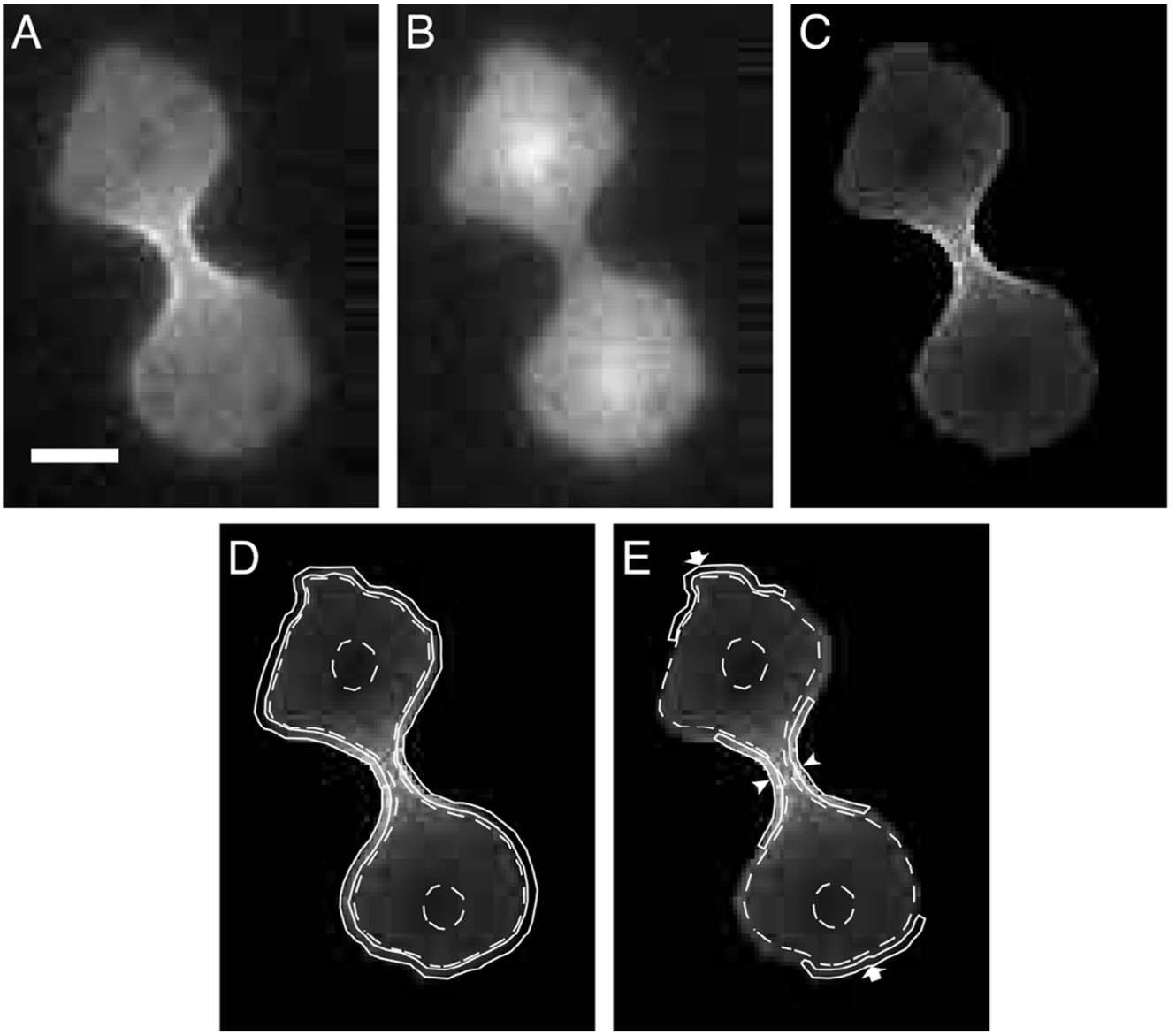

Figure 1
Regions defined for analysis. **A.** A dividing cell is imaged with excitation at 490 nm, showing GFP-myosin-II distribution. **B**. The same cell is imaged with excitation at 405 nm, showing the volume marker, NLS-GFP (nuclear localization signal fused to GFP) distribution. **C.** Division of the image in A with the image in B leads to this resulting ratio image. **D.** The cortex is defined as the 0.35-μm thick shell of the cell, bordered by the solid continuous lines. The cytoplasm (outlined by dashed lines) is the total volume of the cell minus the volume of the cortex. It should be noted that the fluorescence intensity of the cytoplasm in the central region of the cell included the overlying and underlying cortex. However, the contribution of these cortical components to the total fluorescence intensity of the cytoplasmic region was calculated to be less than 2%. The nuclei are encircled to mark their positions, but their combined volume is inconsequential. **E.** The furrow cortex region is indicated with arrowheads and the polar cortex is indicated with arrows. Bar, 5 μm.

The fluoresecent dextran was introduced into the cytoplasm of cells expressing NLS-GFP and GFP-Myosin II by electroporation. Ratio images of GFP-myosin-II were generated using either the dextran or NLS-GFP, as marker of cytoplasmic volume, and the results compared. The myosin-II concentration in the cell cortex measured using NLS-GFP was 96% ± 0.63% (n = 10; all measurements are mean ± SEM) of that measured using the fluorescent dextran. This indicates that the penetration of the cortex by NLS-GFP was as complete as that by the dextran and was

therefore not limited by its size. Therefore, this NLS-GFP is suitable as a cytoplasmic volume marker with the added benefit of serving as an indicator for cells entering mitosis [8]. The NLS-GFP was used as the volume indicator for all subsequent ratio-imaging analyses. Another requirement is that the fluorescence intensity remains uniform over the entire thickness of the sample so that the signal accurately reflects the volume of the sample. We examined the intensity profile emitted by a film of purified recombinant GFP. The fluorescence intensity was constant over a range of several μm above and below the focal plane (data not shown). Thus, the experimental setup is appropriate to determine the concentration of GFP-myosin-II in various compartments of a 10-μm cell. The correction of GFP-myosin-II images by ratio imaging makes a significant difference to the perceived distribution of myosin-II within the cell; in particular, myosin-II is more concentrated in the cell cortex and in the cleavage furrow cortex than is suggested by uncorrected GFP-myosin-II images alone (Figure 1). The intensities recorded in ratio images are proportional to local GFP-myosin-II concentrations and were used to measure the accumulation and dynamics of myosin-II distribution.

Patterns of cortical myosin-II concentration during mitosis and cytokinesis

Both wild type and 3 × Ala myosin-II had a similar flux during mitosis but differed in magnitude. During interphase, wild type myosin-II concentration in the total cortex was 25% ± 1.4% (n = 43) higher than in the cytoplasm while 3 × Ala myosin-II was 44% ± 1.5% (n = 11) higher in the cortex than in the cytoplasm. Entry into mitosis was associated with a drop in cortical myosin-II levels: a 9% ± 1.7% (n = 12) decrease for wild type and 12% ± 2.3% (n = 11) decrease for 3 × Ala myosin-II (measured between interphase and nuclear division). This drop was followed by a period of relatively stable, depressed cortical myosin-II levels that persisted until nuclear division (Figure 2). This decrease may correspond to the mobilization of myosin-II from pre-existing cortical actin-myosin-II structures and may correlate with the redistribution of actin from the cortex to the cytoplasm [16].

Following the onset of anaphase, relative cortical myosin-II concentrations of both proteins rose throughout the periods of anaphase and cleavage furrow progression. They peaked close to the time of daughter cell separation and returned to interphase levels as the daughter cells returned to interphase morphology and behavior (Figure 3).

The relative concentrations of GFP-myosin-II were compared for three regions of cells undergoing cytokinesis: the furrow cortex, the polar cortex and the cytoplasm (Figure 1). Both myosin-II proteins invariably concentrated in the cleavage furrow cortex during cytokinesis, though the 3 × Ala mutant did so to a greater extent. GFP-myosin-II began to concentrate in the cortex of the presumptive furrow near the time of nuclear division, and it continued to rise in this region until the completion of cytokinesis. The peak concentration of wild type GFP-myosin-II was 1.8 ± 0.14 relative to the polar cortex and 2.0 ± 0.14 relative to the cytoplasm (n = 12). In contrast, the peak concentration of 3 × Ala GFP-myosin-II was 6.2 ± 0.36 (n = 11) relative to the cytoplasm and 7.5 ± 0.49 (n = 11) relative to the cortex at the poles. After separation of the daughter cells, the concentration of both myosin-II proteins inherited by their posterior ends declined but remained elevated over polar concentrations for several minutes.

Conversion of the concentration ratios into real fractional amounts of total myosin-II at different stages of cytokinesis

To convert the concentration ratios into real amounts of myosin-II, the volumes of each of the cellular compartments (cleavage furrow cortex, total cortex and cytoplasm) were calculated (Table 1). To do this, we modeled the cell in three shapes: a sphere at early anaphase, a cylinder with two spherical caps at late anaphase, and a dumbbell with spherical cap domains connected by a cylindrical intercellular bridge. Then, by considering that the total amount of myosin-II in the cell is 100%, the percentage of myosin-II in the furrow can be calculated at any point during division. Even though there is little or no volume change during cytokinesis, it should be noted that modeling the cell as these simple shapes does not yield perfect agreement in the total calculated volumes between each stage. The volume of the sphere appears 11% less than the volume of the cylinder while the volumes of the cylinder and dumbbell are within 3% of each other. This is probably because the cell is resting on a surface so that in the "spherical" stage it is not perfectly spherical. As the cell shape becomes more complex in the subsequent stages, the divergence from the ideal shapes is less significant and so the calculated volumes are much closer. In either case, this result does not affect our ability to determine how much myosin-II is in each compartment because the concentrations are calculated based on the volume of that particular shape (stage). The summary of these calculations is presented in Table 1 where every concentration ratio is reflected as percentages of total myosin-II.

From this analysis, it becomes apparent that about 75% of the total myosin-II (wild type and 3 × Ala) remains cytoplasmic in interphase and throughout cytokinesis. During cytokinesis, both wild type and 3 × Ala myosin-II increase in total cortical myosin-II by 29% ((27%-21%)/21%) and 25% ((30%-24%)/24%), respectively. This is reminiscent of the 26% increase in total surface area expected if a spherical cell conserved its volume during cytokinesis and could simply reflect passive accumulation as a result of the

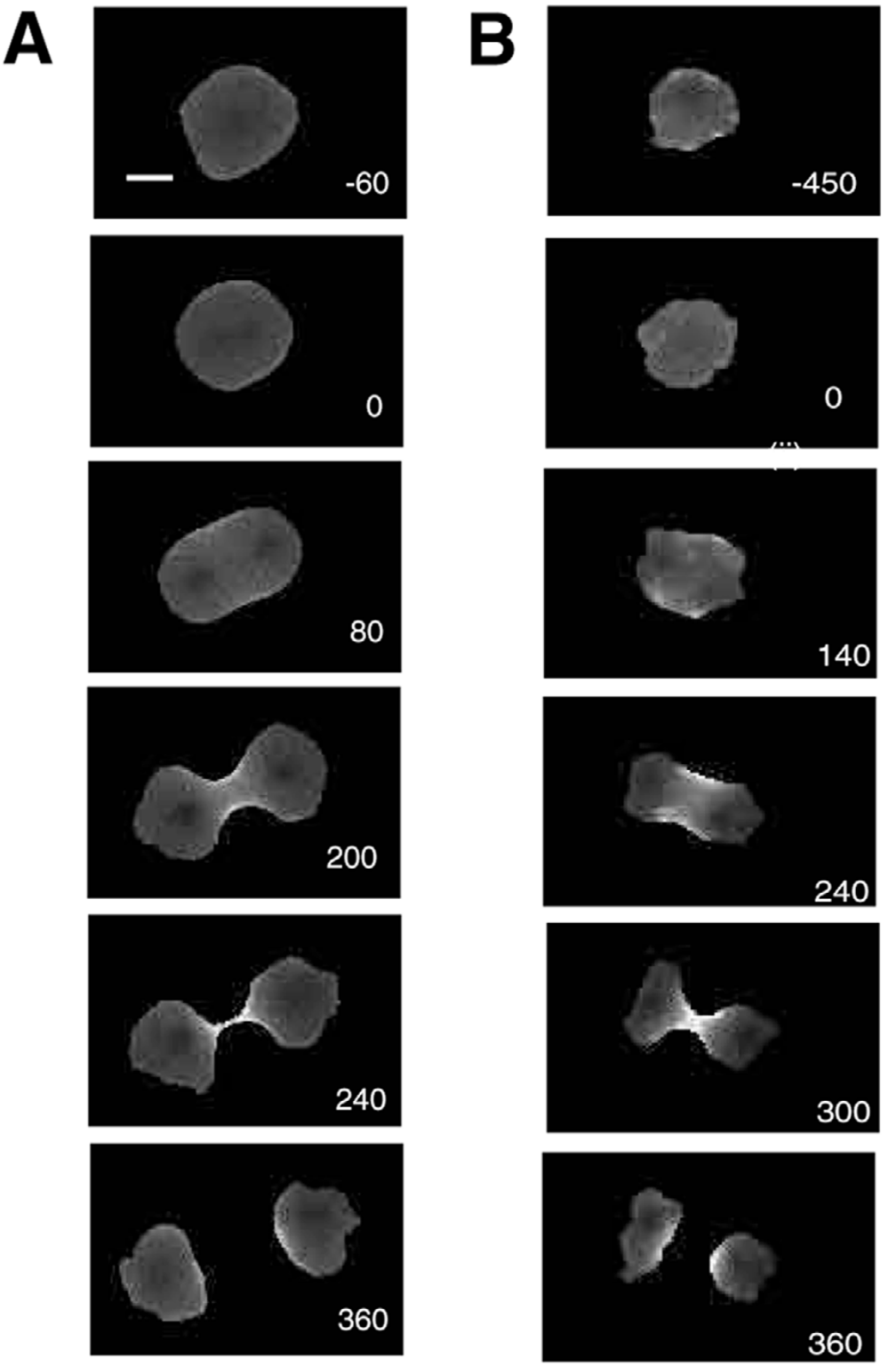

Figure 2
A. A time series of ratio images of a wild type GFP-myosin-II expressing cell going through cytokinesis. The numbers indicate seconds with 0 defined as the point of nuclear division. **B.** A time series of ratio images of a 3 × Ala GFP-myosin-II expressing cell going through cytokinesis. Bar, 5 μm.

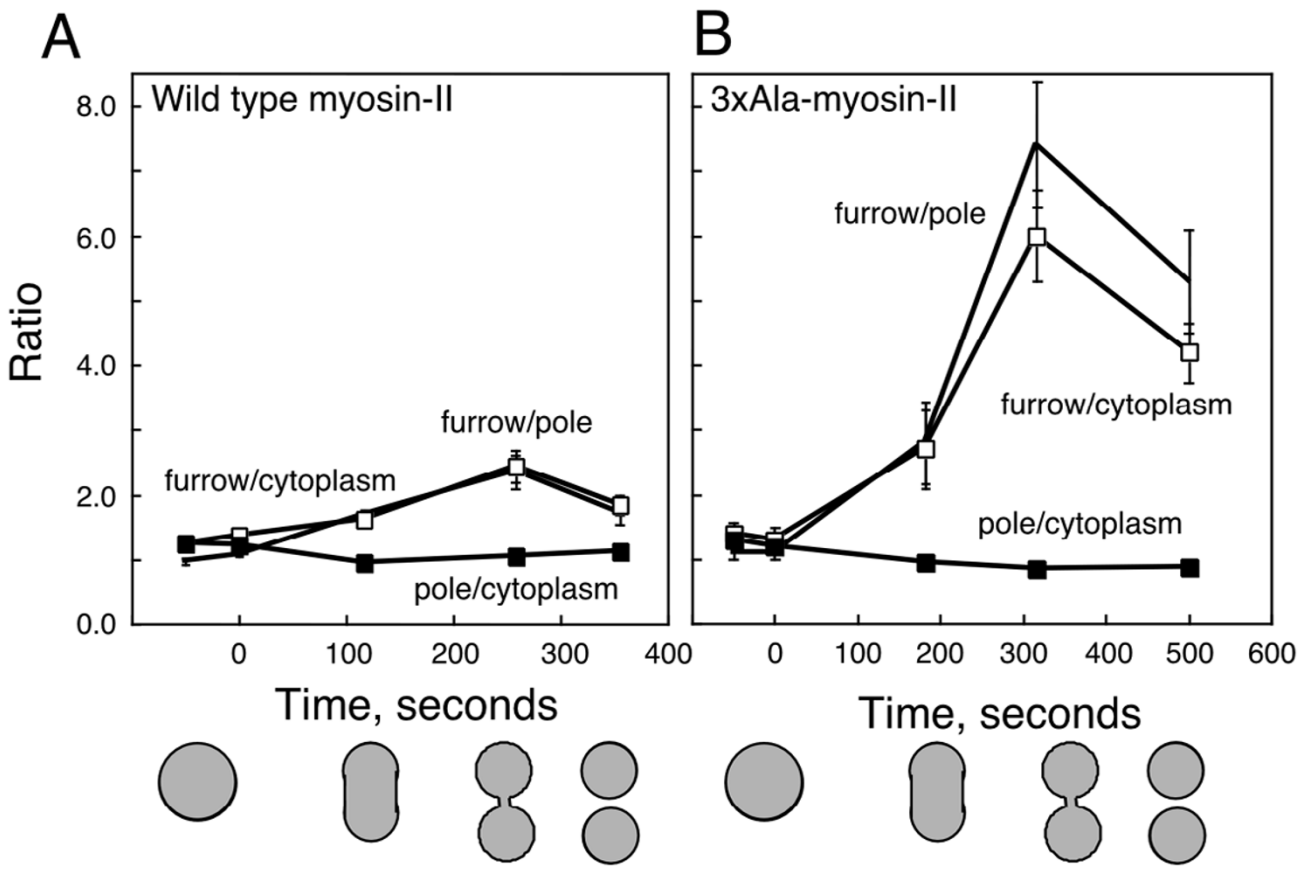

Figure 3
The relative intensity ratios for the pole cortex, furrow cortex and cytoplasm were measured as a function of time. Zero seconds indicates the point of nuclear division. **A.** The graph shows the ratios obtained with wild-type GFP-myosin-II. The shapes of the cells at four different time points are indicated by the cartoons. **B.** This graph shows the ratios obtained with cells expressing 3 × Ala GFP-myosin-II. Standard errors for each time point are based on n≥ 4. Markers: furrow-to-pole, no marker; furrow-to-cytoplasm, open square; pole-to-cytoplasm, closed square. The same markers are used for both plots.

increase in the surface area to volume ratio. During cytokinesis, the amount of wild type myosin-II in the cleavage furrow cortex peaks at the time when the cell is the most cylindrical prior to the ingression of the cleavage furrow. At this point, there is about 8.4% of the cell's myosin-II (about 1×10^5 hexameric monomers) localized to the cleavage furrow cortex. Although the concentration of myosin-II in the cleavage furrow cortex increases as cytokinesis progresses to completion, the amount of myosin-II decreases. This is due to the furrow cortex volume decreasing as cytokinesis progresses. 3 × Ala myosin-II shows a different trend. During cytokinesis, the protein progressively accumulates in the furrow cortex until the cell completes division, indicating that heavy chain phosphorylation normally facilitates removal of wild type myosin-II from the contractile ring.

Where does the cleavage furrow cortex myosin-II originate?

Through this analysis (Table 1), it becomes apparent that only a few percent of the total cellular myosin-II has to move to account for the observed distributions. The first movement occurs between interphase and the spherical stage (onset of nuclear division) in which 2% of the total wild type and 3% of the total 3 × Ala myosin-II are released from the cortex to the cytoplasm. From the spherical stage to the cylindrical stage the amount of total cortical myosin-II remains constant. For wild type myosin-II, if the cortical protein were evenly distributed in the total cortex, 6.5% of the protein would already exist in the region of the furrow cortex with similar amounts in each polar cortex. To get the 8.4% that are observed at the furrow cortex, 2% of the total cellular myosin-II must move to the furrow cortex region. Approximately, 1% of total cellular myosin-II departs from each polar cortex (approximately 13% of the total in the polar cortex), sug-

Table 1: Quantitation of myosin-II distribution during cytokinesis : Comparison with minimal force requirements.

	Interphase	Spherical	Cylindrical	Dumbbell
Cell volume, μm^3 [a]	620	620	690	720
Volume of cell cortex, μm^3 [a]	120	120	130	160
Volume of furrow, μm^3 [a]	-	-	40	20
Total wild type myosin-II, % total [μM]	100 [3.4]	100 [3.4]	100 [3.4]	100 [3.4]
Cytoplasm[b]	77 ± 2 [3.2]	79 ± 2 [3.4]	79 ± 2 [3.4]	73 ± 2 [3.2]
Total cortex[b]	23 ± 0.3 [4.0]	21 ± 0.5 [3.6]	21 ± 0.5 [3.8]	27 ± 0.5 [4.2]
Furrow cortex[b]	**-**	**-**	**8.4 ± 0.2 [5.0]**	**5.3 ± 0.4 [6.4]**
Total 3 × Ala myosin-II, % total [μM]	100 [3.4]	100 [3.4]	100 [3.4]	100 [3.4]
Cytoplasm[b]	74 ± 2 [3.2]	77 ± 2 [3.2]	76 ± 8 [3.2]	70 ± 4 [3.0]
Total cortex[b]	26 ± 0.8 [4.6]	23 ± 0.5 [4.0]	24 ± 1 [4.4]	30 ± 0.1 [4.6]
Furrow cortex[b]	**-**	**-**	**13 ± 1 [7.6]**	**16 ± 1 [18]**
Minimal force requirements, nN[c]	-	-	7.2	2.7
% of total myosin-II required for this amount of force[d]	**-**	**-**	**12**	**4.5**

[a] These quantities were calculated based upon the geometry and dimensions of the cell. [b] These quantities were calculated from the empirically determined concentrations derived from the ratio imaging analysis. [c] These quantities were calculated based upon the dimensions of the cell. [d] These quantities were calculate by considering the amount of minimal required force, the physical properties of myosin-II and the amount of myosin-II in the cell.

gesting that the flux of myosin-II may be from the polar cortices to the cleavage furrow cortex. Similar types of movements are observed for the 3 × Ala myosin-II. To begin, 7% of the 3 × Ala myosin-II would be expected at the furrow cortex if the total cortical 3 × Ala myosin-II were evenly distributed. Then, an additional 6% of the cell's 3 × Ala myosin-II is recruited to the furrow cortex at the expense of the polar cortex.

As the cell progresses from the cylindrical stage to the dumbbell stage, the amount of wild type myosin-II in the cortex increases from 21% to 27% of the total cellular myosin-II. The concentration of myosin-II in the polar cortex increases by 10% while the concentration in the furrow cortex increases by 26%. This indicates that the total cortex gains myosin-II but the furrow cortex gains myosin-II at a faster rate. Similarly, the amount of 3 × Ala myosin-II localized to the cortex also increases from 24% to 30% of the total cellular myosin-II. However, in this case, the polar cortex actually decreases its concentration of myosin-II by 18% while the furrow cortex increases its concentration by 250% during this interval. Thus, for the transition from the cylinder to dumbbell stage, the flux of wild type and 3 × Ala myosin-II must come largely from the cytoplasm to the cortex and myosin-II is recruited into the furrow cortex at the expense of the polar cortex. One way to think of these results is that myosin-II might diffuse into the new cortex volume as the cell increases its surface area and myosin-II in the thick filament form is then recruited to the furrow cortex.

Estimation of the minimal force requirements for cytokinesis

To relate the amount of cleavage furrow myosin-II to the potential forces that might be generated by the cleavage furrow cortex, we estimated the minimal force requirements for cell cleavage using the simple mathematical relationship proposed by Yoneda and Dan [4]. While oversimplified, the results from this analysis provide a basic framework for conceptualizing the meaning of our quantitative distribution and flux analyses. To justify applying the Yoneda and Dan equation (equation 1; Materials and Methods), certain assumptions must be met. One assumption is that the volume is conserved during cell division. Greenspan [17] described the theoretical cell shape changes that occur if conservation of cell volume is maintained. In this regime, the region of the cortex proximal to the cleavage furrow will constrict while the polar cortex expands. The proximal and distal regions intersect, producing stationary rings. We overlaid sequential images of a dividing cell and indeed stationary rings are observed (Figure 4A). It can be seen that the cross-sectional diameter of the emerging daughter cells remains relatively constant if drawn where the stationary rings have formed (Figure 4B). Further, as predicted by the conservation of volume assumption, the pole-to-pole distance increases as the furrow radius decreases (Figure 4B).

By measuring the cell dimensions and using measured interphase cortical stiffnesses (1.55 nN/μm) [9,10], we calculated the minimal required force for a dividing cell at each stage using equations 1–3 (Figure 4C, 4D; Table 1; see Methods). From this analysis, the peak force require-

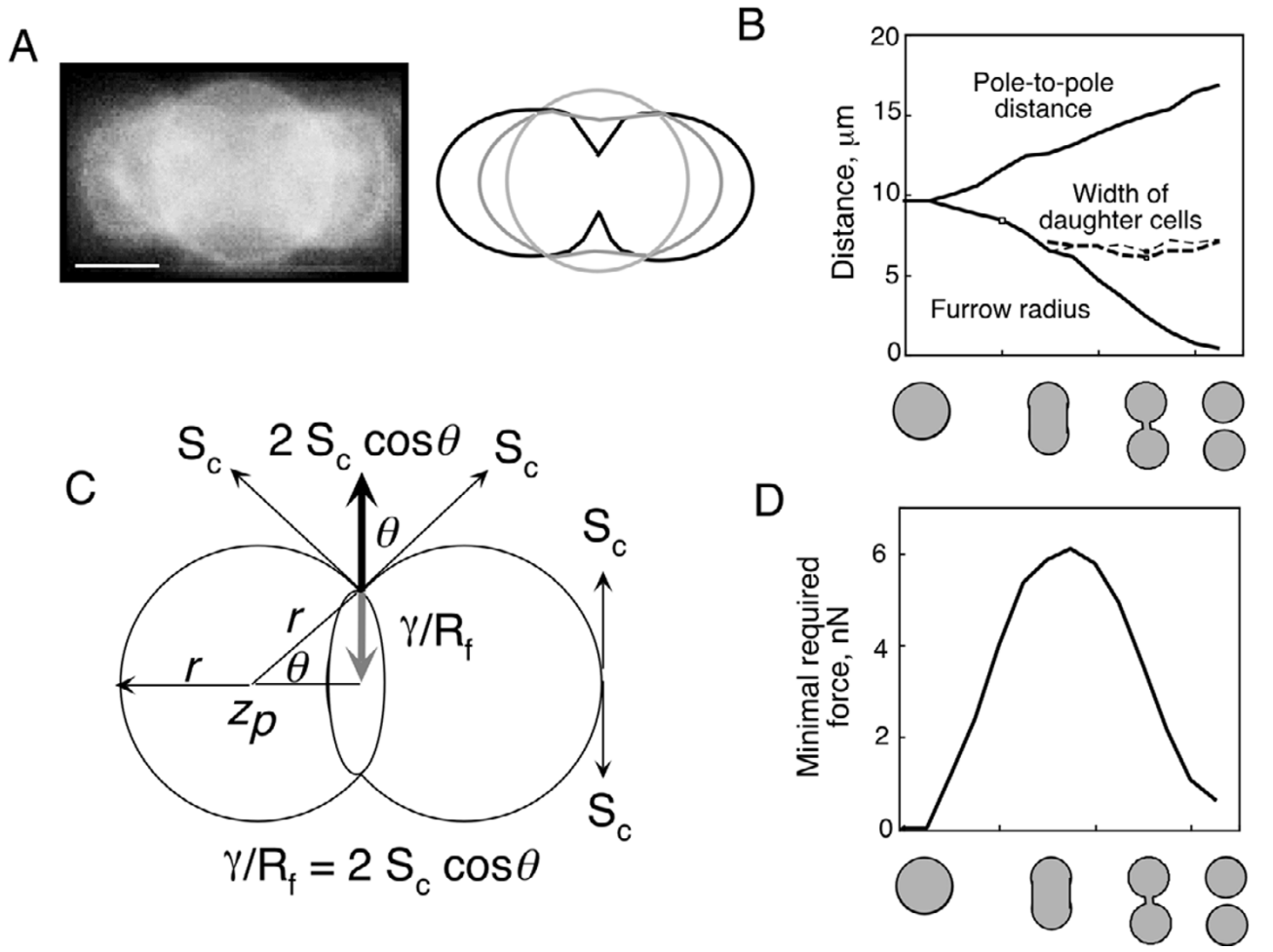

Figure 4
A. An overlay of micrographs of sequential stages of a dividing *D. discoideum* cell expressing GFP-dynacortin [30]. Stationary rings are apparent. The cartoon highlights the shape of the cell cortex during the sequential shape changes. Bar, 5 μm. **B.** The pole-to-pole distance increases as the cleavage furrow radius decreases. As soon as the emerging daughter cells become distinguishable, their cross-sectional diameters remain constant until the completion of division. **C.** The vectors that were calculated to relate the contractile force to the cortical stiffness. The radius of the furrow is also the radius of curvature of the ingressing furrow cortex and γ is the minimal required contractile force if the cortical stiffness is S_c. **D.** The minimal estimated force required at any point of division is plotted as a function of cell shape.

ment occurs when the cell acquires a cylindrical shape. This level of force persists until the point when the radius of the furrow begins to constrict beyond the radius of the emerging daughter cells. After this time, the cleavage furrow continues to ingress, which results in cell shapes that require progressively less contractile force to maintain. By the time the cell has assumed a dumbbell shape, the required contractile force is nearly one third of that required during the cylindrical shape stage.

The amount of myosin-II required to produce the needed force at each point during division was estimated by considering the physical properties and cellular concentration of myosin-II (see Methods). We performed these calculations to approximate the amount of myosin-II required at each stage of division (Table 1). About 10% of the total cellular myosin-II are required in the cylindrical shape and the amount decreases to about 5% by the dumbbell shape. The amounts and trends predicted from the simple Yoneda and Dan equation [4] are in close agreement to the amounts and trends measured by ratio imaging (Table 1).

Discussion

Myosin-II localization is the result of a dynamic steady state in which recruitment is offset by thick filament dis-

assembly. In this model, a signal that possibly emanates from the mitotic spindle instructs the cortex to recruit myosin-II to the furrow cortex and to begin contraction. This leads to the elongation of the cell to the cylindrical form followed by constriction of the furrow. Myosin-II is recruited until enough protein has accumulated and the cell can constrict in the desired manner. More myosin-II is recruited to the furrow cortex when *D. discoideum* cells are flattened by agar overlay when compared to cells grown under standard conditions on the surface of a culture plate [18]. Flattening a cell by agar overlay may increase the apparent stiffness of the cell by introducing tension into the cortex from increased hydrostatic pressure. Intriguingly, myosin-II null *D. discoideum* cells divide relatively normally if allowed to adhere to a surface [8], but myosin-II becomes essential if the adherent cells are grown under a sheet of agarose [19].

The pathway for myosin-II disassembly is most likely always active and the direction of the steady state depends on whether the signal to recruit myosin-II is active. Consistent with this concept, Yumura [20] measured the turnover of cortically distributed myosin-II by fluorescence recovery after photobleaching (FRAP) and showed that wild type myosin-II is localized to the cortex with a half-life of about 7 seconds. This cortical half-life is the same regardless of whether the cell is in interphase or undergoing cytokinesis. On the other hand, the 3 × Ala mutant myosin-II has a half-life greater than the several minutes used to track the protein. The quantitation of the distribution of the 3 × Ala GFP-myosin-II verifies that phosphorylation-controlled disassembly is a normal part of myosin-II turnover. The amount of the 3 × Ala myosin-II enrichment in the furrow cortex might represent normal accumulation of myosin-II that is ordinarily offset by the disassembly of the myosin-II thick filaments possibly as a part of a feedback mechanism that senses the mechanical needs of the cell.

The data presented here does not distinguish between recruitment of myosin-II to the cleavage furrow cortex by cortical sliding or recruitment from the cytoplasm. Between the period of cytokinesis involving transition from a spherical cell shape to a cylindrical shape, there is little or no net flux of myosin-II from the cytoplasm to the cortex. A simple interpretation is that the myosin-II simply slides along the cortex from the poles to the cleavage furrow. Indeed, FRAP studies support a model where dynamic myosin-II filaments progressively slide along the cortex while exchanging with the cytoplasmic pool of myosin-II monomers [20]. However, between the cylindrical and dumbbell stages of cell shape, there is a net flux of myosin-II from the cytoplasm to the cortex. This flux from the cytoplasm to the cortex may simply reflect the increase in the surface area (and consequently the cortex volume) to total cell volume ratio and may not be specific to cytokinesis per se. Then, cortical flow could continue to concentrate the myosin-II into the furrow cortex. Since more 3 × Ala myosin-II than wild type myosin-II is recruited to the cleavage furrow cortex, the recruitment mechanism is unlikely to be limiting for the wild type myosin-II. This suggests that an unlimiting regulator molecule may control the localization of myosin-II. A candidate for a catalytic regulator molecule is the PAKa kinase, which is required for myosin-II localization to the cleavage furrow cortex [21]. This kinase could act on enzymes that regulate the myosin-II assembly-state or it could act on a cortical receptor for myosin-II thick filaments.

During cytokinesis, global and spatial mechanical properties are likely used to deform a cell, allowing the constriction of the cell's equator (reviewed in [22]). These spatial properties include local modulation of stiffness and the generation of contractile force. A localized stiffness increase may define the region that is deformed during a morphological process. The cleavage furrow cortex increases in stiffness above the global stiffness in mammalian cells as determined by atomic force microscopy [23]. This regional increase in stiffness is likely to occur in most or all metazoan and ameboid cells. For example, in *D. discoideum*, the cortexillin actin-filament crosslinking proteins are recruited to the cleavage furrow where they are thought to contribute to the stiffness of the cleavage furrow cortex [24,25]. Myosin-II is probably a major contractile force generator. However, direct measurement of this parameter is far more difficult in small cells. In this paper, we have measured the amount of myosin-II that is recruited to the cleavage furrow cortex. This amount is in close agreement with the estimate of the amount of myosin-II that would be required to generate the forces that may be required to cleave a cell.

The mechanical model presented provides a useful framework for conceptualizing the quantitation of myosin-II. However, there are many issues that must be considered before a comprehensive model for contractile force production can be developed. First, it should be noted that myosin-II null cells can divide if given a surface to which to adhere. The mechanism by which these cells divide under these conditions is not known. However, by considering the mechanics of the process one realizes that the cell has the highest need for force generation during elongation and initial furrow ingression. Traction forces may serve well to elongate the cell, allowing the formation of the cylindrical shape. Indeed, myosin-II null cells in the absence of surface attachment fail to elongate, verifying that myosin-II is required for this step when surface traction is not available [8]. Other gelation and solvation factors and possibly an unconventional myosin might complete the process once the cylindrical shape has been

acquired (for further discussion see [3]). Interestingly, during interphase the myosin-II null cells are 30% less stiff in bending modulus and 70% less stiff in surface tension than the wild type parental cells [10,26]. Thus, by considering the mechanics of division, one realizes that myosin-II null cells probably require significantly less force to divide, making it easier to cleave. Since other proteins are likely to contribute to contractile force production, the quantitation of the amount of myosin-II recruited to the cleavage furrow cortex allows us to estimate how much force can be provided by myosin-II. In fact, there are adequate amounts of myosin-II to generate at least the majority of the forces that are estimated to be required. It is reasonable that the contractile ring may be able to generate greater force than is minimally required. Having the ability to generate more force than is minimally required may have great utility in nature. Environmental factors such as cell-cell contact and hypotonicity might place additional demands on the equatorial contractile apparatus that go beyond the intrinsic stiffness of the cell cortex.

Another issue is that the level of myosin-II activity may be able to vary. In muscle, there is load-dependent recruitment of myosin-II cross-bridges; in other words, the duty ratio of muscle myosin-II can vary (reviewed by [27]). For our calculations, we considered the duty ratio to be 0.006, which is the value measured for unloaded *D. discoideum* myosin-II. Load-dependent recruitment of crossbridges for *D. discoideum* myosin-II has not been examined so it is not known whether this is important for a simple eukaryotic nonmuscle myosin-II. However, this ratio may be able to change in a load-dependent manner such that the amount of myosin-II that is recruited to the cleavage furrow may be able to generate much greater forces than appear to be minimally required. Myosin-II activity might also be predicted to vary as a result of localized activation by myosin light chain phosphorylation. However, in *D. discoideum*, myosin light chain phosphorylation is not required for cytokinesis so this is unlikely to be a major consideration [28,29]. Finally, the ratio imaging experiments do not allow us to make conclusions regarding the radial uniformity of the myosin-II in the cleavage furrow cortex. Thus, it is possible that the force generation is not generated in a perfectly symmetrical fashion. However, the contractile force may not need to be generated in an entirely uniform manner to generate the needed forces to stabilize the ingression of the cleavage furrow cortex. The quantitation of amounts of myosin-II that are recruited to the contractile ring is an essential starting point for developing a more detailed but experimentally tractable model for cytokinesis. Given the complex bookkeeping involved in accounting for the contributions of each individual force generator to the precise mechanical needs of every individual cell, it is remarkable that the trends of myosin-II distribution are so closely predicted by the simple theoretical analysis.

Conclusion

Direct measurements of the cortex stiffness and contractility as a function of position and time during cytokinesis in wild type and mutant cells will be essential to identify the contribution of myosin-II to the mechanics of cell shape changes. Examination of the effects of other proteins that are involved in cytokinesis such as the cortexillins [24,25] and dynacortin [30] will also be necessary to understand how different factors contribute to the different mechanical parameters such as stiffness and contractility. It should be remembered that in this study the agreement between the amount of myosin-II required in the cleavage furrow cortex determined from Hooke's law and the amount measured using ratio imaging is strictly correlative. What is most notable, however, is that the trends predicted from the simple model accurately predict the trends of myosin-II recruitment to the cleavage furrow cortex. Other more sophisticated models for cytokinesis have been presented [31]. However, the value of this simple theoretical analysis is that it more accurately predicts the trends of contractility, which may be assigned in large part to myosin-II and it can be easily tested in a variety of cell types for its validity. If it generally provides reliable estimates of the mechanical considerations for dividing cells, it would be a useful tool for researchers who are interested in quantitative approaches to studying the biology of cytokinesis.

Materials and Methods

DNA manipulation and cell culture

All DNA manipulations were carried out using standard procedures [32] unless otherwise specified. GFP-myosin-II and NLS-GFP were simultaneously expressed from the same extrachromosomal plasmid vector (p102 in the case of wild-type GFP-myosin-II, p122 in the case of 3 × Ala GFP-myosin-II). To generate p102, the coding region of Bex1 GFP [15] was subcloned into pBS-MyBam [33]. The fusion of GFP to the N-terminal region of the myosin-II heavy chain gene was subsequently subcloned into pBig-MyD. The coding region of Vex1 GFP [15] was subcloned into pDXA-3C [34] as described [8], and the NLS-GFP expression cassette subcloned into p102. p122 was made by replacing the 3' region of the myosin-II heavy chain gene in p102 with the equivalent fragment from pBIG-ALA [5].

All constructs were transformed into the parental JH10 strain or HS1, a myosin-II heavy chain (*mhcA*$^-$) null strain [13], unless otherwise indicated. Cells were cultured in DD-Broth20 [34] with the addition of 100 μg/ml thymidine for JH10 and 10 μg/ml G418 for plasmid selection. The pLD1A15SN:GFP-dynacortin plasmid was transformed into DH1 cells and the cells were grown in Hans'

Enriched HL-5 with 7.5 μg/ml G418 [30]. For experiments with Texas Red-dextran, the fluorescent dextran was electroporated into cells.

Microscopy

For microscopic observation, cells were plated in chambered coverslips (Nalge Nunc) for 2 hours in fresh medium, washed once with Imaging Buffer (20 mM MES pH 6.8, 25 mM potassium chloride, 2 mM magnesium sulfate, 0.2 mM calcium chloride) and covered with 1.5 ml of the same buffer. Observations were made with a Zeiss Axiovert 100TV with Plan-Apo 63x/1.4 NA objective (Carl Zeiss Inc.). Fluorescence images from 30–50 ms exposures were recorded using a TE/CCD-512TKB camera and ST-138 controller (Princeton Instruments Inc.) and manipulated with Image 1/Metamorph (Universal Imaging Corp.).

Fluorescence images were collected with triple bandpass dichroic (450–485 nm, 510–550 nm and 590–650 nm transmitted; Chroma Tech. Corp.) and Hi-Q FITC emission filter (510–560 nm transmitted; Chroma Tech. Corp.). Pairs of images of Bex1 and Vex1 GFPs were recorded in rapid succession (<500 ms) by switching bandpass excitation filters between 479–501 nm and 398–413 nm using a Lambda 10–2 filter wheel controller (Sutter Instrument Co.).

Ratio image analysis

Image processing was in three principal steps: background subtraction, correction for spectral overlap and ratio generation. Mean background signal was measured in a region of each image unpopulated by cells and subtracted from the entire image. Spectral overlap was measured in cells expressing only one of the two GFP variants. These measurements showed that the intensity of the Bex1 signal using a Vex1 excitation filter was 0.11 ± 0.0054 (n = 44; all measurements are mean ± SEM) of the Bex1 signal using a Bex1 excitation filter. Further, the intensity of the Vex1 signal using a Bex1 excitation filter was 0.027 ± 0.00057 (n = 50) of the Vex1 signal using a Vex1 excitation filter. These measurements allowed the contributions of each GFP to the image intended to represent the other GFP to be subtracted out. Division of the corrected GFP-myosin-II image by the corrected NLS-GFP image yielded ratio images with pixel intensities that are proportional to local myosin-II concentrations (except in the region occupied by the nucleus).

Four regions of dividing cells were defined for analysis purposes: the cortex as a whole, the cytoplasm, the cortex underlying the cleavage furrow and the cortex underlying the poles (Figure 1). The cytoplasm was defined as the entire contents of the cell excluding the cortex and the nuclei. The cortex was defined as a layer with a constant thickness of 0.35 μm. This number is justified because the thickness of cortical GFP-myosin-II fluorescence is approximately 0.35 μm and is consistent with published electron micrographs of *D. discoideum* cell cortices [35]. It should be noted that fluorescence that is defined as cytoplasm also includes fluorescence from the overlying and underlying cortices. However, this amount of cortex contributes less than 2% of the total fluorescence of the cytoplasm, which is within the error of the cytoplasmic concentration measurement (Table 1) and is, therefore, negligible.

The furrow and polar cortical regions were each subsets of the cortex as defined above. The cortex underlying the furrow is considered to extend outwards from the equator as far as the point of inflection of the curvature of the cell (Figure 1). This region corresponds well to the most advanced part of the furrow and to the region in which myosin-II is concentrated. This region also contains the contractile ring actin filaments [36]. The polar cortex is defined as the two cortical regions furthest from the equator, these regions being of equivalent size to the furrow region as defined above (Figure 1E). Regions of interest were drawn manually onto images and their mean pixel intensities were recorded and processed in Excel (Microsoft). Graphical representations were generated in KaleidaGraph (Synergy Software).

To convert the ratios of myosin-II into quantities, the volumes of each of the cell regions of were calculated from the cell's dimensions. First, the total cell volume was determined. Then, the cytoplasm volume was calculated by considering the dimensions of the whole cell minus the cortex and the cortex volume was calculated as the difference between the total cellular volume and the cytoplasm volume. To calculate the furrow cortex volume at the cylinder stage, the furrow was considered to be the "belt" that constricts in subsequent time points. At the cylinder stage it was determined to be 30% of the cell's total length. The volume of the furrow cortex was calculated as a difference between the outer cell cylinder and the inner cytoplasmic cylinder. At the dumbbell stage, the cleavage furrow cortex volume was calculated as the sum of its parts (see Figure 1E). First, the intercellular bridge was modeled as the difference between the inner and outer cylinders. The portion of the furrow cortex flanking the intercellular bridge, which extend upwards to the flexion point of the curvature of the main cell body, was modeled as a difference of inner and outer spherical caps. The small fraction of this volume where the intercellular bridge intersects the spherical caps was subtracted from the furrow cortex volume.

To determine the fraction of myosin-II in any compartment, the concentration of myosin-II in the furrow cortex was c, the concentration in the cytoplasm was $c \bullet$ (1/ratio

of furrow cortex to cytoplasm), and the concentration in the polar cortex was c • (1/ratio of furrow cortex to polar cortex). Then, the sum of the products of the concentrations of each part multiplied by that part's volume equals 100% of the myosin-II in the cell. Once c is solved for algebraically, the concentrations of each part can be determined and the fraction of the total cellular myosin-II in each region is the product of the concentration and the region's volume.

Analysis of Cell Geometry and Calculation of Minimal Force Requirements

To analyze the cell geometry during cytokinesis, dimensions of dividing *D. discoideum* cells were measured using NIH Image to determine the number of pixels for a particular dimension. Calculations were made with Excel (Microsoft Corp.).

To calculate the minimal required force to cleave a cell, we used Yoneda and Dan's equation [4]:

$$\gamma/R_f = 2S_c(\cos\Theta) \qquad \text{Equation 1}$$

where γ is the contractile force, R_f is the radius of the furrow, S_c is the stiffness of the cell cortex and Θ is the angle between the tangent to the cortex at the base of the furrow and the cleavage plane (Figure 4C). We considered S_c to be 1.55 nN/μm, which was measured using a microcapillary aspiration technique [9,10]. To calculate the balance of forces using the equation proposed by Yoneda and Dan [4], the in-plane stiffness or surface tension is the appropriate parameter to consider. The glass needle indentation method [26] has also been used to measure the cortical stiffness of *D. discoideum*. However, this method mostly measures the bending modulus.

To determine the minimal force requirements of cells undergoing cell division, we analyzed movies of dividing *D. discoideum* cells. The diameter of the cleavage furrow ($2R_f$) and the pole to pole distance ($2Z_p$) were measured. The radius (r) of each emerging daughter cell was calculated using the following:

$$r = (Zp^2 + Rf^2)/2Z_p \qquad \text{Equation 2}$$

Then, Cos(Θ) was calculated from the following:

$$\cos(\Theta) = (Zp - r)/r \qquad \text{Equation 3}$$

The contractile force was then calculated by inputting the various quantities and solving for γ. Parameters were plotted versus cell shape (which change as a function of time) to demonstrate how the minimal required contractile force varied as a function of cell shape.

The amount of myosin-II required to produce a particular amount of force was calculated by assuming that a single head of myosin-II produces 3.5 pN of force [12]. To correct for myosin-II's duty ratio (t_s/ t_c), the following considerations were used. The maximum velocity (V) for translation of actin filaments by *D. discoideum* myosin-II is 3.3 μm/s [13] and the step size is 8 nm [14]. If V equals the step size divided by the strongly bound state time (t_s), then t_s equals 8 nm/3300 nm/s or about 2.4 msec. The V_{max} for the actin-activated myosin-II ATPase cycle is about 2.5 s^{-1}[14]. Therefore, the total cycle time (t_c) is about 400 msec. Thus, the duty ratio is about 0.006 for *D. discoideum* myosin-II. For comparison, the duty ratio for vertebrate skeletal myosin-II is about 0.05 [11].

To determine the percentage of total cellular myosin-II, the following assumptions were used to calculate the total amount of myosin-II in a cell: total protein concentration in *D. discoideum* is 50 μg/10^6 cells [37], myosin-II represents about 1% of the cell's protein [38,39], the relative molecular mass of a hexameric "monomer" (two each of the heavy chain and essential and regulatory light chains) of myosin-II is 557 kDa, and the average size of a *D. discoideum* cell is about 8 μm in diameter when grown on surfaces. To determine the average cell size, cultures were grown on surfaces, resuspended in media, and the population distribution of the cell diameter measured with a Z1 Coulter counter (Beckman Coulter Inc.). From this, an average density of myosin-II per μm^3 was determined to be approximately 2000 monomers per μm^3 (approximately 3.4 μM) so that the amount of myosin-II in any cell with a particular volume could be estimated, assuming that the average concentration remains the same.

Acknowledgements

We thank Michael Brenner (MIT), Wendy Zhang (Harvard), Ivana Nikolic, John Dawson, Wen Liang, Dan Hostetter, and David Altman for helpful discussions and critical comments on the manuscript. This work was supported by the Burroughs Wellcome Fund (DNR) and the National Institutes of Health (#GM404509; JAS).

References

1. Rappaport R: **Cytokinesis in Animal Cells.** *Cambridge, Cambridge University Press* 1996
2. Rappaport R: **Cell division: Direct measurement of maximum tension exerted by furrow of echinoderm eggs.** *Science* 1967, **156**:1241-1243
3. Robinson DN, Spudich JA: **Towards a molecular understanding of cytokinesis.** *Trends Cell Biol* 2000, **10**:228-237
4. Yoneda M, Dan K: **Tension at the surface of the dividing sea-urchin egg.** *J Exp Biol* 1972, **57**:575-587
5. Egelhoff TT, Lee RJ, Spudich JA: ***Dictyostelium* myosin heavy chain phosphorylation sites regulate myosin filament assembly and localization *in vivo*.** *Cell* 1993, **75**:363-371
6. Sabry JH, Moores SL, Ryan S, Zang J-H, Spudich JA: **Myosin heavy chain phosphorylation sites regulate myosin localization during cytokinesis in live cells.** *Mol Biol Cell* 1997, **8**:2605-2615
7. Yumura S, Uyeda TP: **Myosin II can be localized to the cleavage furrow and to the posterior region of Dictyostelium amoebae without control by phosphorylation of myosin heavy and light chains.** *Cell Motil Cytoskeleton* 1997, **36**:313-322

8. Zang J-H, Cavet G, Sabry JH, Wagner P, Moores SL, Spudich JA: **On the role of myosin-II in cytokinesis: Division of *Dictyostelium* cells under adhesive and nonadhesive conditions.** *Mol Biol Cell* 1997, **8**:2617-2629
9. Gerald NJ, Dai J, Ting-Beall HP, DeLozanne A: **A role for *Dictyostelium* RacE in cortical tension and cleavage furrow progression.** *J Cell Biol* 1998, **141**:483-492
10. Dai J, Ting-Beall HP, Hockmuth RM, Sheetz MP, Titus MA: **Myosin I contributes to the generation of resting cortical tension.** *Biophys J* 1999, **77**:1168-1176
11. Uyeda TQP, Kron SJ, Spudich JA: **Estimation from slow sliding movement of actin over low densities of heavy meromyosin.** *J Mol Biol* 1990, **214**:699-710
12. Finer JT, Simmons RM, Spudich JA: **Single myosin molecule mechanics: piconewton forces and nanometre steps.** *Nature* 1994, **368**:113-119
13. Ruppel KM, Uyeda TQP, Spudich JA: **Role of highly conserved lysine 130 of myosin motor domain: *In vivo* and *in vitro* characterization of site specifically mutated myosin.** *J Biol Chem* 1994, **269**:18773-18780
14. Murphy CT, Rock RS, Spudich JA: **A myosin II mutation uncouples ATPase activity from motility and shortens step size.** *Nat Cell Biol* 2001, **3**:311-315
15. Anderson MT, Tjioe IM, Lorincz MC, Parks DR, Herzenberg LA, Nolan GP, Herzenberg LA: **Simultaneous fluorescence – activated cell sorter analysis of two distinct transcriptional elements within a single cell using engineered green fluorescent proteins.** *Proc Natl Acad Sci USA* 1996, **93**:8508-8511
16. Yumura S, Fukui Y: **Spatiotemporal dynamics of actin concentration during cytokinesis and locomotion in *Dictyostelium*.** *J Cell Sci* 1998, **111**:2097-2108
17. Greenspan HP: **On the dynamics of cell cleavage.** *J Theor Biol* 1977, **65**:79-99
18. Neujahr R, Heizer C, Albrecht R, Ecke M, Schwartz JM, Weber I, Gerisch G: **Three-dimensional patterns and redistribution of myosin II and actin in mitotic *Dictyostelium* cells.** *J Cell Biol* 1997, **139**:1793-1804
19. Yumura S, Uyeda TQP: **Transport of myosin II to the equatorial region without its own motor activity in mitotic Dictyostelium cells.** *Mol Biol Cell* 1997, **8**:2089-2099
20. Yumura S: **Myosin II dynamics and cortical flow during contractile ring formation in *Dictyostelium* cells.** *J Cell Biol* 2001, **154**:137-145
21. Chung CY, Firtel RA: **PAKa, a putative PAK family member, is required for cytokinesis and the regulation of the cytoskeleton in *Dictyostelium discoideum* cells during chemotaxis.** *J Cell Biol* 1999, **147**:559-575
22. Robinson DN: **Cell division: Biochemically controlled mechanics.** *Curr Biol* 2001, **11**:R737-740
23. Matzke R, Jacobson K, Radmacher M: **Direct, high-resolution measurement of furrow stiffening during division of adherent cells.** *Nat Cell Biol* 2001, **3**:607-610
24. Weber I, Gerisch G, Heizer C, Murphy J, Badelt K, Stock A, Schwartz J-M, Faix J: **Cytokinesis mediated through the recruitment of cortexillins into the cleavage furrow.** *EMBO J* 1999, **18**:586-594
25. Simson R, Wallraff E, Faix J, Niewöhner J, Gerisch G, Sackmann E: **Membrane bending modulus and adhesion energy of wild-type and mutant cells of *Dictyostelium* lacking talin or cortexillins.** *Biophys J* 1998, **74**:514-522
26. Pasternak C, Spudich JA, Elson EL: **Capping of surface receptors and concomitant cortical tension are generated by conventional myosin.** *Nature* 1989, **341**:549-551
27. Howard J: **Molecular motors: structural adaptations to cellular functions.** *Nature* 1997, **389**:561-567
28. Chen P, Ostrow BD, Tafuri SR, Chisholm RL: **Targeted disruption of the Dictyostelium RMLC gene produces cell defective in cytokinesis and development.** *J Cell Biol* 1994, **127**:1933-1944
29. Ostrow BD, Chen P, Chisholm RL: **Expression of amyosin regulatory light chain phosphorylation site mutant complements the cytokinesis and developmental defects of *Dictyostelium* RMLC null cells.** *J Cell Biol* 1994, **127**:1945-1955
30. Robinson DN, Spudich JA: **Dynacortin, a genetic link between equatorial contractility and global shape control discovered by library complementation of a *Dictyostelium discoideum* cytokinesis mutant.** *J Cell Biol* 2000, **150**:823-838
31. He X, Dembo M: **On the mechanics of the first cleavage division of the sea urchin egg.** *Exp Cell Res* 1997, **233**:252-273
32. Sambrook J, Fritsch EF, Maniatis T: **Molecular Cloning: A Laboratory Manual.** *Cold Spring Harbor, Cold Spring Harbor Press* 1989
33. Moores SL, Sabry JH, Spudich JA: **Myosin dynamics in live *Dictyostelium* cells.** *Proc Natl Acad Sci USA* 1996, **93**:443-446
34. Manstein DJ, Schuster HP, Morandini P, Hunt DM: **Cloning vectors for the production of proteins in *Dictyostelium discoideum*.** *Gene* 1995, **162**:129-134
35. Ogihara S, Carboni J, Condeelis J: **Electron microscopic localization of myosin II and ABP-120 in the cortical actin matrix of *Dictyostelium* Amoebae using IgG-gold conjugates.** *Dev Genet* 1988, **9**:505-520
36. Fukui Y, Inoue S: **Cell division in *Dictyostelium* with special emphasis on actomyosin organization in cytokinesis.** *Cell Motil Cytoskeleton* 1991, **18**:41-54
37. Loomis W: **Genetic tools for *Dictyostelium discoideum*.** *Methods Cell Biol* 1987, **28**:31-65
38. Clarke M, Spudich JA: **Biochemical and structural studies of actimyosin-like proteins from non-muscle cells.** *J Mol Biol* 1974, **86**:209-222
39. Clarke M, Spudich JA: **Nonmuscle contractile proteins: The role of actin and myosin in cell motility and shape determination.** *Ann Rev Biochem* 1977, **46**:797-822